In-situ studies of large magnetostriction in $DyCo_2$ compound by synchrotron-based high-energy x-ray diffraction

Zhihua Nie[1,a)], Zilong Wang[1], Sen Yang[2,b)], Daoyong Cong[3], Yang Ren[4], Dennis E Brown[5] and Yan-dong Wang[3,c)]

[1]School of Materials Science and Engineering, Beijing Institute of Technology, Beijing 100081, China

[2]School of Science, MOE Key Laboratory for Nonequilibrium Synthesis and Modulation of Condensed Matter and State Key Laboratory for Mechanical Behavior of Materials, Xi'an Jiaotong University, Xi'an 710049, China

[3]State Key Laboratory for Advanced Metals and Materials, University of Science and Technology Beijing, Beijing 100083, China

[4]X-Ray Science Division, Argonne National Laboratory, Argonne, IL 60439, USA

[5]Department of Physics, Northern Illinois University, DeKalb, IL 60115, USA

Corresponding authors: zhihua_nie@yahoo.com (Z. Nie), yangsen@mail.xjtu.edu.cn (S. Yang), ydwang@mail.neu.edu.cn (Y.-d. Wang)

Abstract

Synchrotron-based high-energy x-ray diffraction is used to explore the physical origin of large magnetostriction in $DyCo_2$, an RT_2 compound (R = rare earth, T = Co, Fe), by tracing the crystal structural change as a function of temperature and magnetic field. When the $DyCo_2$ compound is zero-field cooled down below the Curie temperature T_C, the high-temperature cubic lattice is distorted into a tetragonal structure, associated with an expansion of unit cell volume. When a magnetic field is applied gradually from 0 to 6 T below T_C, no changes in the peak positions for tetragonal $(800)_T$ and $(008)_T$ peaks are observed, whereas their relative peak intensities are gradually changed. The intensity changes generated during magnetic field increasing are reversed stepwise with decreasing the magnetic field. Our experimental results suggest that the large magnetostriction in $DyCo_2$ is caused by the crystallographic domain-switch mechanism (or rearrangement of tetragonal domains). The diffraction elastic strain is not detected under the field up to 6 T. The present investigations provide a fundamental understanding of the mechanisms of the large magnetostriction in RT_2 compounds with Laves phases.

Keywords: magnetostriction; domain switching; diffraction elastic strain; high-energy x-ray diffraction; $DyCo_2$

1. Introduction

Magnetostriction is a distinct property of magnetic materials, which refers to a deformation in their shape or dimensions in response to a change in magnetization and has broad applications in actuators and sensors [1-2]. Usually, the anisotropic magnetostriction (*Joule magnetostriction*, anisotropic changes in linear dimensions induced by an external magnetic field) in magnetic materials is small [3]. However, RT_2 intermetallic compounds (R = rare earth, T = Co, Fe), one interesting group discovered in the early of 1960s, exhibit a large anisotropic magnetostriction on the order of 0.1% in a moderate saturation field (less than 1 T) below the Curie temperature (T_C) [4-6]. Today, RT_2 compounds are widely employed as high-power transducers that convert energy between magnetic and elastic states.

Recent synchrotron data show that the ferromagnetic transition in RT_2 compound is also a structural transition, yielding a low crystallographic symmetry conforming to spontaneous magnetization [7,8]. The magnetic and structural transitions are coupled in this alloy system; thus, a large magnetocaloric effect is detected during the first-order magneto-structural phase transition [9-11]. The object of the present study is the $DyCo_2$ compound. $DyCo_2$, a RT_2 compound with the Laves phase, undergoes a magnetic transition from a paramagnetic to ferrimagnetic state at $T_C \approx 140$ K, where the coupling between heavy rare-earth Dy- and Co-moments becomes antiparallel [12-14]. By using synchrotron-based high-energy x-ray diffraction (HE-XRD) techniques, we find that the large low-field anisotropic magnetostriction in RT_2 compounds, such as $DyCo_2$, $TbFe_2$ and $Tb_{0.4}Dy_{0.6}Fe_2$ originates from the field-induced domain switching mechanism rather than lattice distortion [15,16]. Based on the concept of field induced crystallographic domain-switching, the relation between the magnetic stress induced by saturating magnetic field and the theoretical saturation magnetostriction has been discussed [15,16]. The immediate question is what happens if further magnetic field (> 1 T) is applied when the sample becomes one single domain and reaches technical saturation. The crystallographic studies on the magnetostriction related with the field-induced diffraction elastic strain or domain

switch under the high magnetic field have rarely been reported. In this work, in-situ HE-XRD experiments are performed to trace the structural evolution of $DyCo_2$ powders as a function of magnetic field up to 6 T. The high temperature cubic lattice is distorted into tetragonal structure when the $DyCo_2$ powders are cooled below T_C. The tetragonal structure remains rigid under the applied magnetic field. Magnetic-field induced diffraction elastic strain is not detected under the applied magnetic field up to 6 T.

2. Experimental

A $DyCo_2$ polycrystalline ingot was prepared by arc melting high-purity Dy and Co in an argon atmosphere. The phase transition properties of the sample were examined using a physical property measurement system (PPMS, Quantum Design). The thermo-magnetization curves were recorded under a fixed magnetic field strength of 0.01 T with a temperature cooling rate of 2 K min^{-1}.

A part of the ingot was crushed into powders in the liquid nitrogen. The powders with particle size less than 100 micron were used for the HE-XRD experiments, which were loaded in a Kapton tube. The Kapton tube was 0.3 mm in diameter. In-situ HE-XRD experiments (with photon energy of 115 keV) were performed at beamline 11-ID-C, Advanced Photon Source, Argonne National Laboratory. The wavelength of used x-ray was 0.108 Å. An Oxford cryomagnet cooled by liquid helium was installed on the beamline to generate magnetic fields up to 6.5 T with temperature control from 4 to 310 K. The Kapton tube with powder sample was fixed on a standard sample holder by Kapton tapes. A thermocouple was screwed near the sample. The direction of the applied magnetic field was aligned perpendicular to the incident x-ray beam and parallel to the horizontal direction. A PerkinElmer α-Si flat-panel large-area detector was used to collect the two-dimensional (2D) diffraction patterns with a sample-to-detector distance of 2.2 meter for achieving a sufficient strain resolution. The experimental layout is described elsewhere [17]. CeO_2 powders were loaded

together with the $DyCo_2$ powders, which were used as a standard for calibrating the sample-to-detector distance under each magnetic field strength.

The software package FIT2D was used for integrating the 2D diffraction patterns along certain azimuth angles to obtain a one-dimensional (1D) diffraction pattern [18]. The general structural analysis software (GSAS) was used for 1D diffraction pattern reduction [19]. Le Bail method was used to determine the temperature-dependent lattice parameters and unit cell volume.

3. Results and discussion

3.1 Structural evolution as a function of temperature

The Curie temperature T_C separates the disordered paramagnetic phase (at $T > T_C$) from the ordered ferromagnetic phase (at $T < T_C$) and is the temperature below which spontaneous magnetization occurs. Fig. 1 presents the thermo-magnetization curves of the polycrystalline $DyCo_2$ under a magnetic field of 0.01 T. The increase in the magnetization observed upon cooling corresponds to the magnetic transition from a paramagnetic to a ferrimagnetic state. The temperature-dependent lattice parameters of the $DyCo_2$ powders were obtained by crystallographic refinement using the Le Bail method, as shown in Fig. 2a. The cubic lattice parameter (a) decreases linearly when the sample is cooled from 300 to 150 K. The tetragonal lattice parameters can be well determined below T_C. The tetragonal distortion is attributed to the anisotropically shaped electron charge cloud expressed by single ion crystal field theory [20].

The unit cell volume of the $DyCo_2$ powders is shown in Fig. 2b as a function of temperature. Upon cooling below T_C, the volume is significantly expanded. In the macroscopic view, when the $DyCo_2$ sample cooled to T_C, a dimension change (spontaneous magnetostriction, λ_0) is observed via thermal expansion measurements [21]. In the microscopic view, unit cell expansion is confirmed here using HE-XRD. This volume change is caused by ordering of the magnetic moments at the onset of ferromagnetism [22]. Invar-like behavior (dimension invariance) is observed in the unit cell volume versus temperature curve (see Fig. 2b), the same as in the thermal

expansion curve after the first-order magnetic transition [21]. The observed invar-like behavior may be related to two magnetic states, i.e., a low-spin low-volume state and a high-spin high-volume state [23].

3.2 Structural evolution as a function of magnetic field strength

Fig. 3 shows the variations of the diffraction patterns for (800) as a function of the magnetic field strength at 30 K in the direction parallel to the field. The diffraction patterns (black circles) can be fitted by a double peak function, which represents the tetragonal $(800)_T$ and $(008)_T$ diffraction peaks. The fitting curves (pink and blue solid lines) and the peak positions (pink and blue dashed lines) are depicted in Fig. 3. Following the visual guides of the dashed lines, it can be clearly observed that the peak positions of $(800)_T$ and $(008)_T$ do not shift upon increasing the magnetic field strength. However, as observed in Fig. 3a, the intensity of the $(800)_T$ peak gradually decreases upon increasing the magnetic field strength from 0 to 0.9 T, and the peak almost disappears when the magnetic field strength is greater than 0.9 T at 30 K. In contrast, the $(008)_T$ peak intensity is progressively enhanced upon increasing the magnetic field strength from 0 to 6 T. Fig. 3b shows the variations of the diffraction patterns for $(800)_T$ and $(008)_T$ from 6 to 0 T. The intensity changes generated during magnetic field increasing are reversed stepwise with decreasing the magnetic field.

The intensity changes of $(800)_T$ and $(008)_T$ diffraction peaks have been quantitatively studied. Fig. 4 shows the $(800)_T$ and $(008)_T$ diffraction peak intensities and the intensity fraction of the $(008)_T$ diffraction peak $[I_{008_T}/(I_{800_T} + I_{008_T})]$ as a function of the magnetic field strength at 30 K. As shown in Fig. 4a, the peak intensity for $(008)_T$ increases gradually when the magnetic field is increased from 0 to 6 T. The $(800)_T$ intensity becomes weakened with increasing the field. For the initial state (0 T, before applying the magnetic field), the fraction of the $(008)_T$ peak intensity is ~ 0.33 (see Fig. 4b). The $(008)_T$ integrated intensity fraction reaches 0.96 when the magnetic field strength is 0.9 T. As shown in Fig. 4c, the peak intensity for $(008)_T$ decreases with decreasing the field. The $(800)_T$ peak appears at 0.8 T and is enhanced when

further decreasing the magnetic field strength. The $(008)_T$ integrated intensity fraction reaches 0.46 when the magnetic field strength is decreased to 0 T, as shown in Fig. 4d.

As demonstrated in Fig. 3, under the applied magnetic field, the diffraction peak positions for $(800)_T$ and $(008)_T$ do not shift as a function of magnetic field strength. Thus, the unit cell of the tetragonal structure remains rigid under the applied magnetic field even up to 6 T. A systematic variation in the diffraction peak intensities is clearly observed when the magnetic field is applied to the $DyCo_2$ powders (see Fig. 4). The sample investigated here is the $DyCo_2$ powders, which are composed by small crystallites (or particles). In the microscopic view, the crystallite can be polycrystalline, which contains some crystal grains. Inside each grain, different low-symmetry crystal domains exhibit for the temperature below T_C. The two magnetostriction mechanisms, i.e., the preferred selection of domains or the rotation of crystallites, need to be discussed comprehensively under the field. The total intensity ($I_{800_T} + I_{008_T}$) keep constant when the magnetic field is increased from 0 to 0.9 T, which suggests that the crystallite rotation can be ignored under the low magnetic field. The different changes in peak intensities, i.e., a decrease of $(800)_T$ peak intensity and an increase of $(008)_T$ peak intensity from 0 to 0.9 T, are attributed to the preferred arrangement of domains (domain-switch mechanism) [15,16].

The (800) diffraction pattern has a high q-value, which lead to a high reciprocal resolution. Therefore, the tetragonal $(800)_T$ and $(008)_T$ diffraction peaks are clearly distinguished (see Fig. 3). However, for the diffraction patterns with a low q-value, their tetragonal patterns are overlapped. Fig. 5 and Fig. 6 show the variations of the diffraction patterns for (422) as a function of the magnetic field strength at 30 K in the direction parallel to the field (Fig. 5) and the direction perpendicular to the field (Fig. 6). As shown in Fig. 5 and Fig. 6, the tetragonal $(422)_T$ and $(224)_T$ diffraction peaks are overlapped very much, which look like a ‘single peak’. The ‘single peak’ seams to shift to a high 2-theta angle under the application of a parallel magnetic field from 0 to 1 T (see Fig. 5). When a perpendicular magnetic field is applied from 0 to 1 T, the

‘single peak’ shifts to a low 2-theta angle (see Fig. 6). In fact, the shift of the ‘single peak’ is attributed to the intensity changes of $(422)_T$ and $(224)_T$ diffraction peaks. The fitting curves (pink and blue solid lines) and the peak positions (pink and blue dashed lines) for the tetragonal $(422)_T$ and $(224)_T$ diffraction peaks are depicted in Fig. 5 and Fig. 6.

3.3 Mechanism of the large magnetostriction in $DyCo_2$ compound

The crystallographic domain-switch mechanism is schematically illustrated in Fig. 7. Fig. 7 (paramagnetic state) presents one possible orientation of the crystal grain aligned with [010] parallel to the incident x-ray beam and [100] parallel to the horizontal. During the first order magnetic transition, the tetragonal distortion of the cubic lattice results in a complex microstructure with multiple domains in $DyCo_2$. One of three cubic axes can be contracted, and the other two are elongated (see Fig. 2). Thereby, in principle, there are three types of crystal domains in the ferrimagnetic state generated from one cubic crystal grain, as illustrated in Fig. 7 (demagnetized state). The three types of variants are denoted domain I, II and III for convenience and correspond to a contraction of the [001], [010] and [100] axes, respectively. The $(800)_T$ diffraction peaks in Fig. 3 are generated from both domain I and domain II, for which the *a*-axis is parallel to the diffraction vector. However, the diffraction intensity for the $(008)_T$ peak originates only from domain III. The ferrimagnetic $DyCo_2$ compound has a long-range ordered magnetic structure with easy magnetization direction $\boldsymbol{M_S}$ along the *c*-axis of the tetragonal structure [7], which is highlighted in red (see Fig. 7, demagnetized state). According to the cryomagnet setup in the experiments, the magnetic field is applied parallel to the horizontal axis and along the [100] axis of the peculiar crystal grains. Therefore, the easy magnetization direction of domain I or II is perpendicular to the field, while that of domain III is parallel to the field. The increase of the integral intensity for $(008)_T$ and decrease for $(800)_T$ as a function of magnetic field strength (see Figs. 4a and 4b) suggest that domain III with the easy magnetization direction parallel to the field is enhanced, whereas domain I

and II with the easy magnetization direction perpendicular to the field are consumed when a magnetic field is applied (see Fig. 7, magnetized state). In fact, the growth of the field-preferred domain enables the reorientation of the magnetization in the field [24,25]. The *c*-axis of the tetragonal domain is shorter than *a*- and *b*-axes (see Fig. 2a). In this case, a growth of the field preferred domain (i.e., domain III with the short axis parallel to the field and long axes perpendicular to the field) at the expense of others will lead to the magnetostriction with a negative $\lambda_{\parallel}$ and a positive $\lambda_{\perp}$ (see Fig. 7, magnetized state).

The $(008)_T$ integrated intensity fraction increases to 0.96 in powders when the magnetic field strength reaches 0.9 T (see Fig. 4b), which suggests that the domain switching has been almost saturated below 1 T [26,27]. Normally, the technical saturation of magnetization is achieved when a magnetic material is converted into a single magnetic domain. At higher fields, the magnetization increases slowly beyond technical saturation, which is called forced magnetization. Our samples are powders. The $(008)_T$ diffraction peak intensity keeps increasing beyond 1 T (see Fig. 4a, 1 - 6 T). It suggests that with increasing the field larger than 1 T, other crystallites are continuously rotated to the specific direction with the *c*-axis orientated along the applied field. The easy magnetization direction $\boldsymbol{M_S}$ is the *c*-axis. Thus, the magnetization of the sample keeps increase with increasing the magnetic field strength. However, the situation is different when the sample is in bulk state [12]. In bulk sample, under a small magnetic field, similar to powers, the magnetization increases because of the domain switching in grains (the first step of 180° domain switching). When the field is further increased after technical saturation, the single domain in grains is forced to rotate by external field. In powder sample, the rotation of single domain is achieved by the rotation of crystallites. In comparison, the rotation of single domain is achieved by the second step of 180° domain switching in bulk sample. Take $DyCo_2$ bulk compound with tetragonal domains for example, the first step of 180° domain switching leads to a negative magnetostriction parallel to the field. And the magnetostriction curve goes upwards direction when the field is further

increased beyond 1 T, which is attributed to the second step of 180° domain switching [28].

4. Conclusions

We have investigated the structural evolution of $DyCo_2$ compound as a function of temperature and magnetic field using the synchrotron-based high-energy x-ray diffraction technique. When the $DyCo_2$ compound is zero-field cooled down below the Curie temperature, the high temperature cubic lattice is distorted into a tetragonal structure, which is associated with an expansion of the unit cell volume. The variations of the diffraction patterns for (800) and (422) are analyzed as a function of the magnetic field strength at 30 K. The magnetostriction in $DyCo_2$ originates from a crystallographic domain-switch mechanism (rearrangement of tetragonal variants). Field-induced diffraction elastic strain is not observed under the applied magnetic field up to 6 T. The magnetization process is discussed in two sample states, i.e., powder sample and bulk sample.

ACKNOWLEDGEMENTS

This work was supported by the National Natural Science Foundation of China (Grant No. 51571032) and the State Key Laboratory for Advanced Metals and Materials (Grant No. 2015-ZD01). Use of the Advanced Photon Source was supported by the U. S. Department of Energy, Office of Science, Office of Basic Energy Sciences, under Contract No. DE-AC02-06CH11357.

References

1. G. Engdahl, Handbook of Giant Magnetostrictive Materials (Academic, San Diego, CA, 2002).
2. M. J. Dapino, in Encyclopedia of Smart Materials, edited by M. Schwartz (Wiley, New York, 2002) Vol. 1-2.
3. J. P. Joule, Philos. Mag. 30 (1847) 76-87.
4. S. N. Jammalamadaka, G. Markandeyulu, K. Balasubramaniam, J. A. Chelvane, J. Alloys Compd. 624 (2015) 40-43.
5. Y. Liu, Q. Wang, T. Liu, P. F. Gao, Y. Yuan, J. C. He, J. Alloys Compd. 590 (2014) 110-115.
6. Z. J. Zuo, D. A Pan, Y. M. Jia, J. J. Tian, S. G. Zhang, L. J. Qiao, J. Alloys Compd. 587 (2014) 287-289.
7. S. Yang, X. B. Ren, Phys. Rev. B 77 (2008) 014407.
8. S. Yang, H. Bao, C. Zhou, Y. Wang, X. Ren, Y. Matsushita, Y. Katsuya, M. Tanaka, K. Kobayashi, X. Song, and J. Gao, Phys. Rev. Lett. 104 (2010) 197201.
9. N. K. Singh, P. Kumar, K. G. Suresh, A. K. Nigam, A. A. Coelho, and S. Gama, J. Phys.: Condens. Matter 19 (2007) 036213.
10. S. Ma, W. B. Cui, D. Li, N. K. Sun, D. Geng, X. Jiang, and Z. D. Zhang, Appl. Phys. Lett. 92 (2008) 173113.
11. D. H. Wang, S. L. Tang, H. D. Liu, W. L. Gao, and Y. W. Du, Intermetallics 10 (2002) 819.
12. A. del Moralt and D. Melville, J. Phys. F: Met. Phys. 5 (1975) 1767.
13. E. W. Lee and F. Pourarian, Phys. Stat. Sol. (a) 33 (1976) 483.
14. N. Ishimatsu, H. Maruyama, N. Kawamura, Y. Ohishi, and O. Shimomura, Nucl. Instrum. Methods Phys. Res. B 238 (2005) 167.
15. Z. H. Nie, S. Yang, Y. D. Wang, Z. L. Wang, D. M. Liu, and Y. Ren, Appl. Phys. Lett. 103 (2013) 111903.
16. Z. H. Nie, S. Yang, Y. D. Wang, Z. L. Wang, D. M. Liu, Y. Ren, T. Y. Chang, and R. Zhang, J. Alloys Compd. 658 (2016) 372-376.
17. D. M. Liu, Z. H. Nie, G. Wang, Y. D. Wang, D. E. Brown, J. Pearson, P. K. Liaw,

and Y. Ren, Mater. Sci. Eng. A 527 (2010) 3561.

18. A. P. Hammersley, “FIT2D: An Introduction and Overview”, ESRF Internal Report, ESRF97HA02T, 1997.
19. C. Larson and R. B. Von Dreele, “General structure analysis system (GSAS)”, LANL Report No. LAUR 86-748, Los Alamos National Laboratory, Los Alamos, NM, 2000.
20. E. Callen and H. B. Callen, Phys. Rev. 139 (1965) A455.
21. R. Grössinger and H. Müller, Rev. Sci. Instrum. 52 (1981) 1528.
22. P. Bean and D. S. Rodbell, Phys. Rev. 126 (1962) 104.
23. M. Schilfgaarde, I. A. Abrikosov, and B. Johansson, Nature 400 (1999) 46.
24. J. X. Zhang and L.Q. Chen, Acta Mater. 53 (2005) 2845.
25. R. D. James and D. Kinderlehrer, J. Appl. Phys. 76 (1994) 7012.
26. Y. Higuchi, H. Sugawara, Y. Aoki, and H. Sato, J. Phys. Soc. Jap. 69 (2000) 4114.
27. A. Kowalczyk, J. Baszynski, A. Szajek, J. Kovac, and I. Skorvanek, J. Magn. Magn. Mater. 152 (1996) L279-L281.
28. M. Adil, S. Yang, M. Mi, C. Zhou, J.Q. Wang, R. Zhang, X.Q. Liao, Y. Wang, X.B. Ren, X.P. Song, and Y. Ren, Appl. Phys. Lett. 106 (2015) 132403.

Figure captions

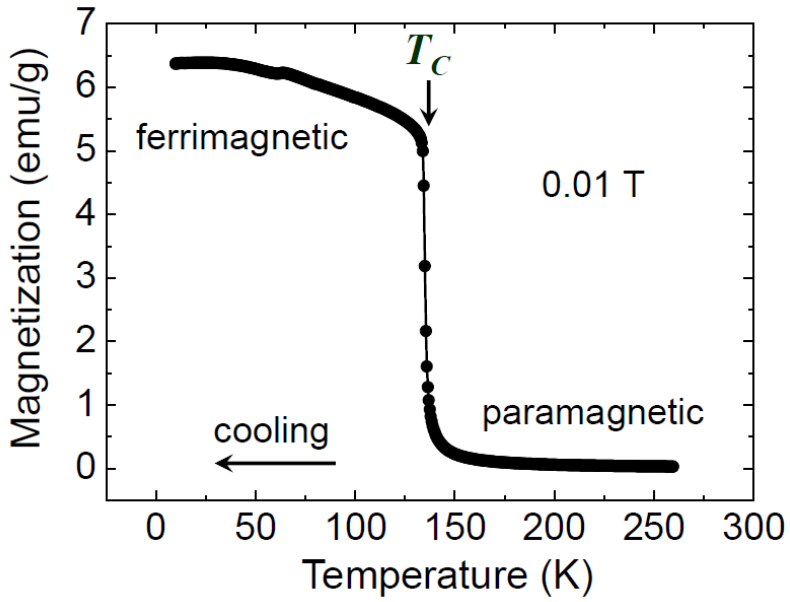

Figure 1

Thermo-magnetization curve (cooling process) of the polycrystalline $DyCo_2$ crystal under a magnetic field of 0.01 T.

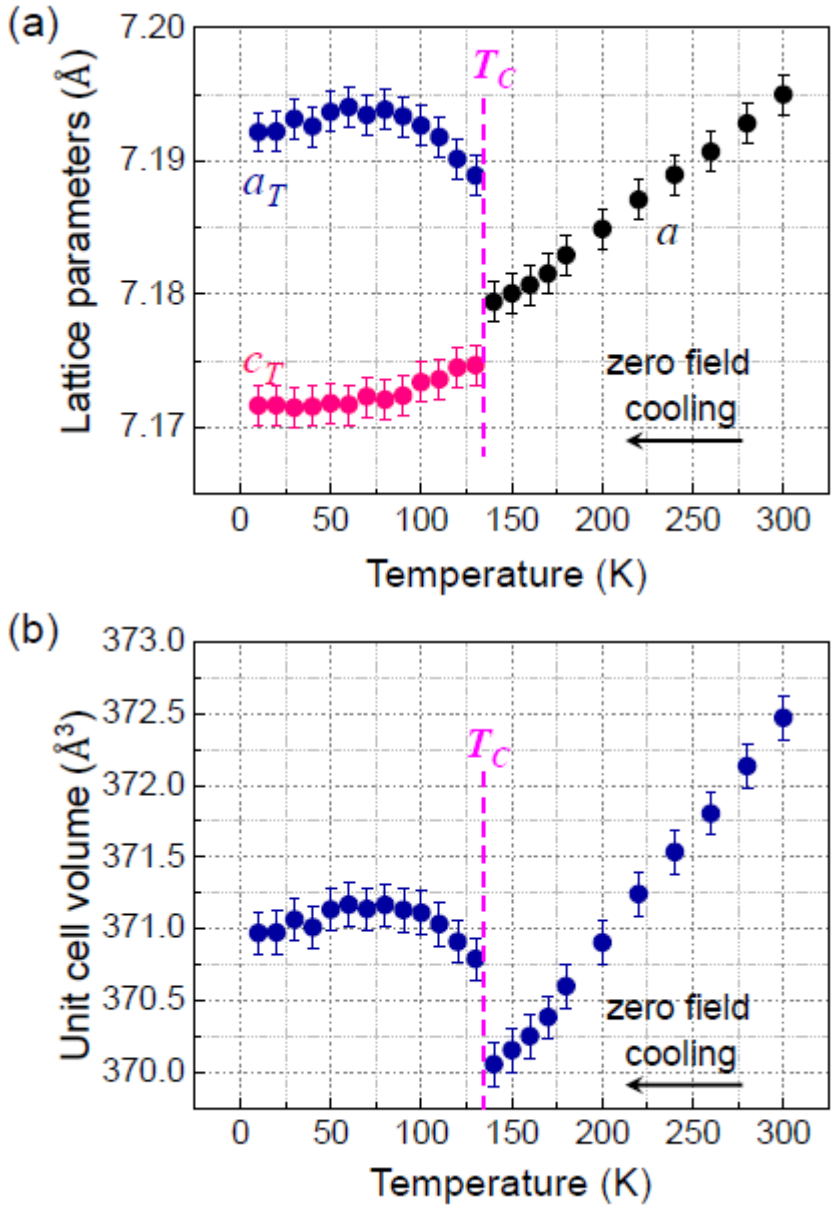

Figure 2

Structural variations of the $DyCo_2$ powders zero-field cooled from 300 to 10 K: (a) lattice parameters; (b) unit cell volume.

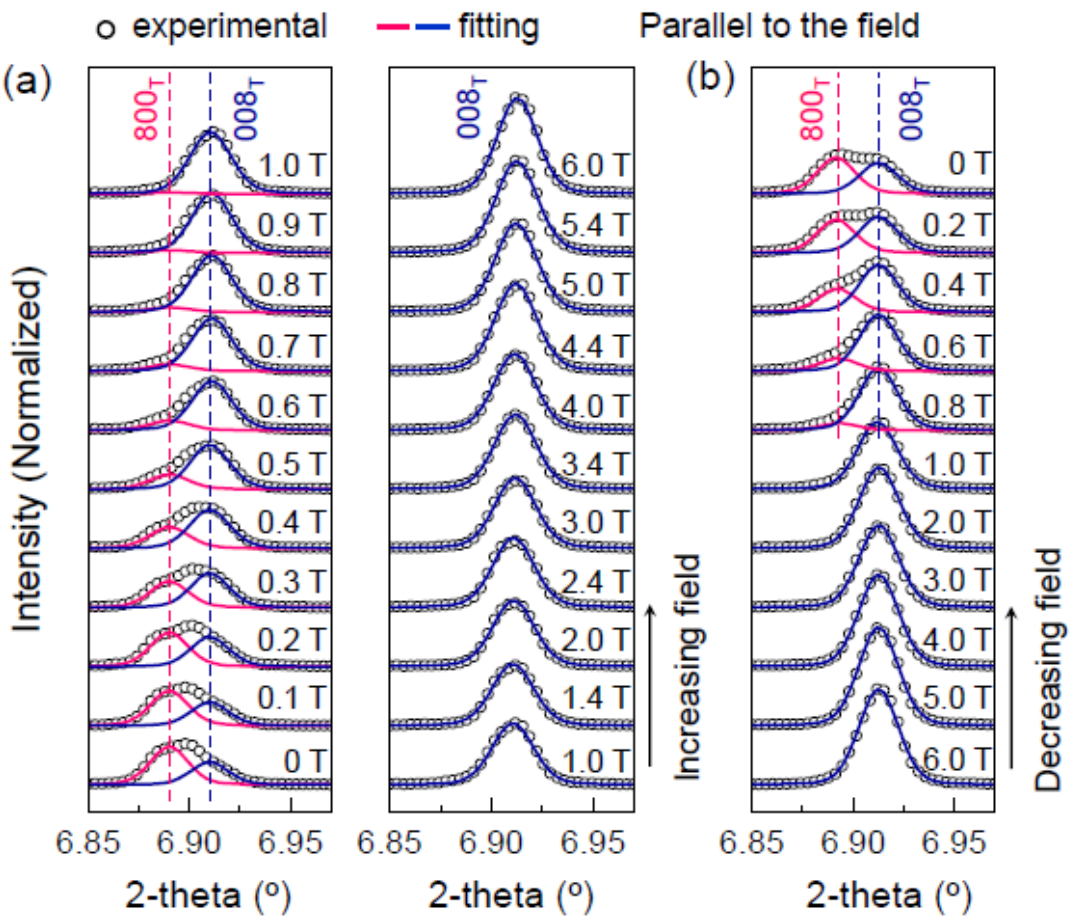

Figure 3

Variations of the $(800)_T$ and $(008)_T$ diffraction peaks under various magnetic field strengths at 30 K, parallel to the field: (a) 0 - 6 T; (b) 6 - 0 T.

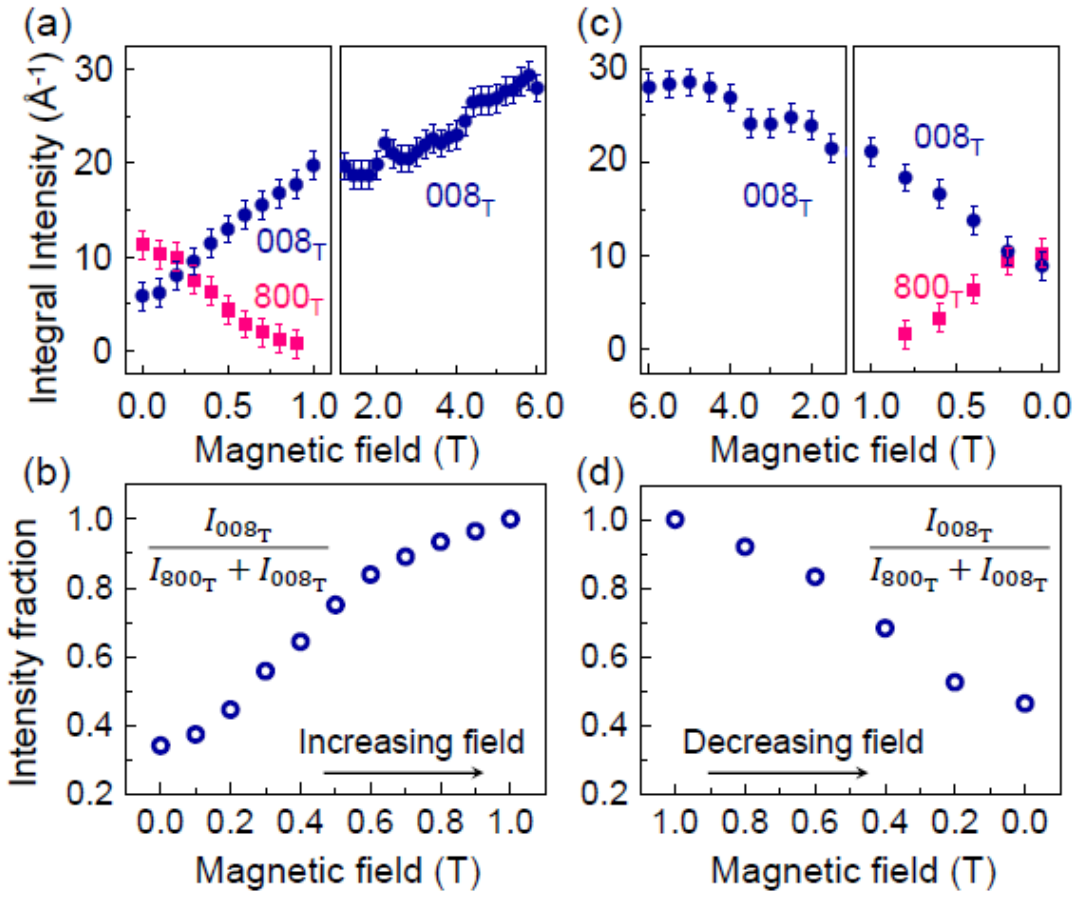

Figure 4

Variations of the $(800)_T$ and $(008)_T$ diffraction peak intensities under various magnetic field strengths at 30 K.

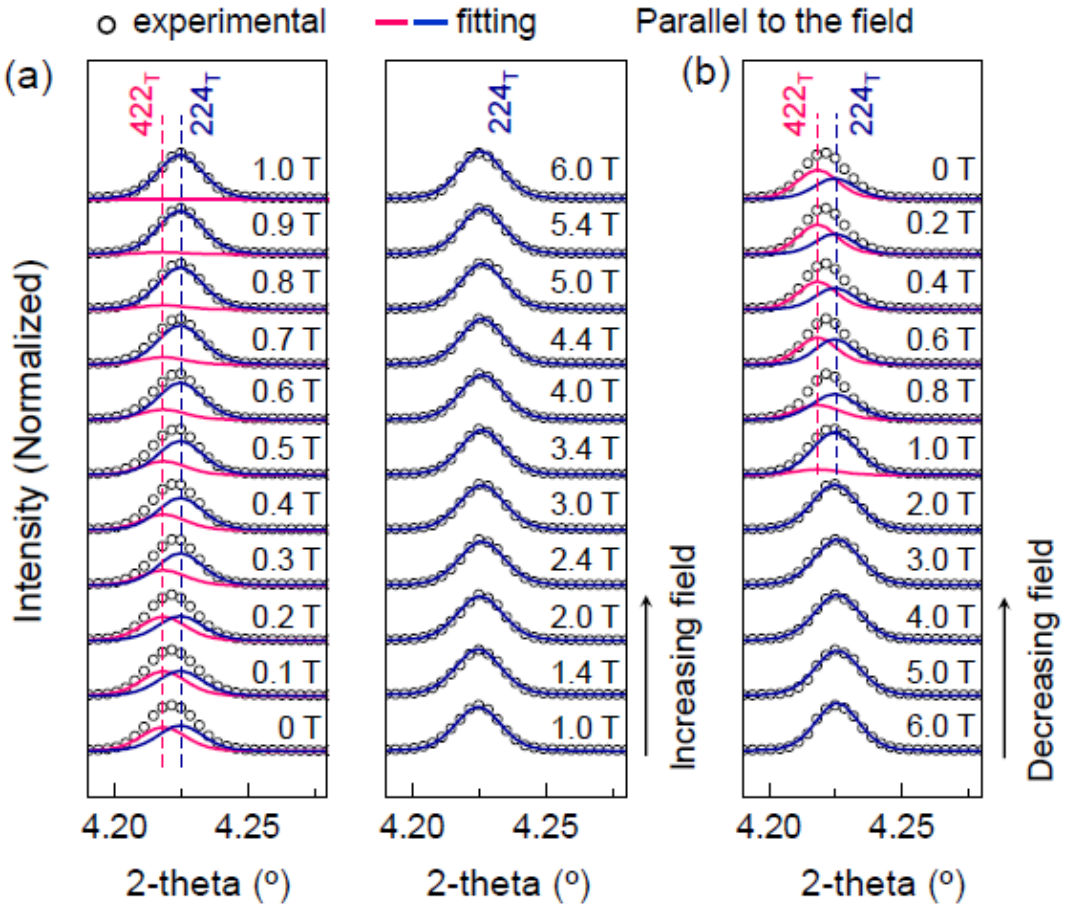

Figure 5

Variations of the $(422)_T$ and $(224)_T$ diffraction peaks under various magnetic field strengths at 30 K, parallel to the field: (a) 0 - 6 T; (b) 6 - 0 T.

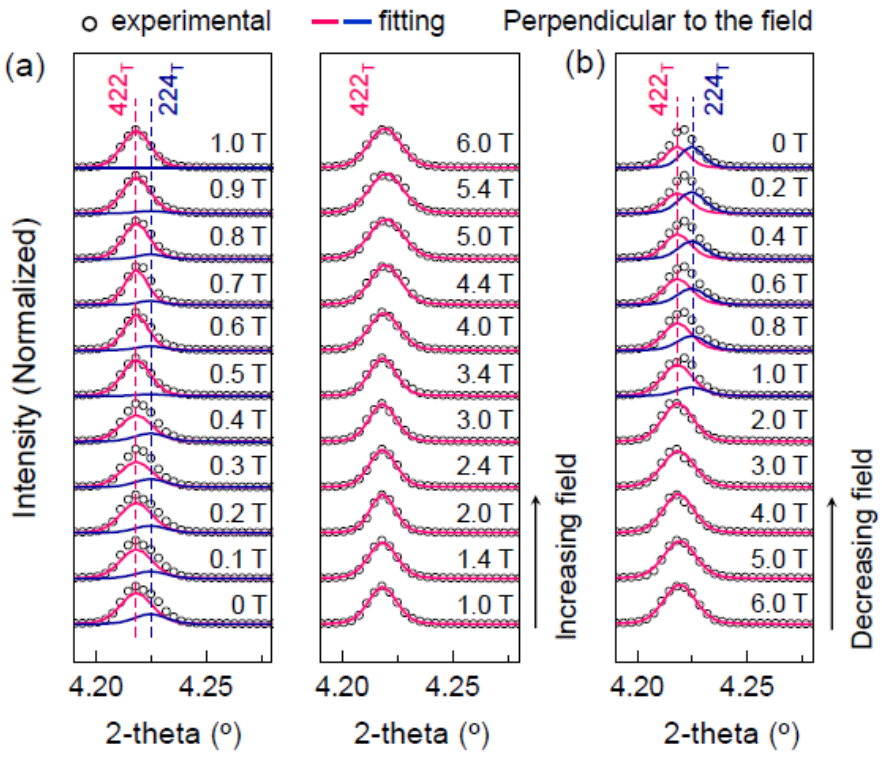

Figure 6

Variations of the $(422)_T$ and $(224)_T$ diffraction peaks under various magnetic field strengths at 30 K, perpendicular to the field: (a) 0 - 6 T; (b) 6 - 0 T.

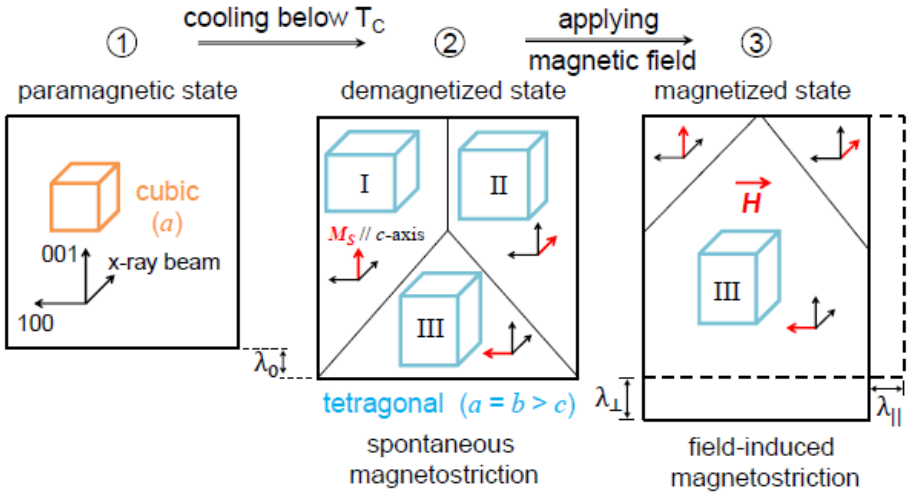

Figure 7

A schematic illustration of the microstructural evolution in $DyCo_2$ compound under magnetic field below the Curie temperature T_C.